OXFORD

SOT | Society of Toxicology
www.toxsci.oxfordjournals.org

TOXICOLOGICAL SCIENCES, 158(1), 2017, 164–175

doi: 10.1093/toxsci/kfx081
Advance Access Publication Date: April 27, 2017
Research article

Blinded Contractility Analysis in hiPSC-Cardiomyocytes in Engineered Heart Tissue Format: Comparison With Human Atrial Trabeculae

Ingra Mannhardt,[*,†] Alexandra Eder,[*,†] Berengere Dumotier,[‡] Maksymilian Prondzynski,[*,†] Elisabeth Krämer,[*,†] Martin Traebert,[‡] Klaus-Dieter Söhren,[*,†] Frederik Flenner,[*,†] Konstantina Stathopoulou,[*,†] Marc D. Lemoine,[*,†,§] Lucie Carrier,[*,†] Torsten Christ,[*,†] Thomas Eschenhagen,[*,†] and Arne Hansen[*,†,1]

[*]Department of Experimental Pharmacology and Toxicology, Cardiovascular Research Center, University Medical Center Hamburg-Eppendorf, 20246 Hamburg, Germany; [†]DZHK (German Center for Cardiovascular Research), Partner Site Hamburg/Kiel/Lübeck, 20246 Hamburg, Germany; [‡]Novartis Pharma AG, CH-4002 Basel, Switzerland; and [§]Department of Cardiology-Electrophysiology, University Heart Center, 20246 Hamburg, Germany

[1]To whom correspondence should be addressed at Department of Experimental Pharmacology and Toxicology, University Medical Center Hamburg-Eppendorf, Martinistrasse 52, 20246 Hamburg, Germany. Fax: (49) 40-741054876. E-mail: ar.hansen@uke.de.

ABSTRACT

Human-induced pluripotent stem cell-derived cardiomyocytes (hiPSC-CM) may serve as a new assay for drug testing in a human context, but their validity particularly for the evaluation of inotropic drug effects remains unclear. In this blinded analysis, we compared the effects of 10 indicator compounds with known inotropic effects in electrically stimulated (1.5 Hz) hiPSC-CM-derived 3-dimensional engineered heart tissue (EHT) and human atrial trabeculae (hAT). Human EHTs were prepared from iCell hiPSC-CM, hAT obtained at routine heart surgery. Mean intra-batch variation coefficient in baseline force measurement was 17% for EHT and 49% for hAT. The PDE-inhibitor milrinone did not affect EHT contraction force, but increased force in hAT. Citalopram (selective serotonin reuptake inhibitor), nifedipine (LTCC-blocker) and lidocaine (Na^+ channel-blocker) had negative inotropic effects on EHT and hAT. Formoterol (beta-2 agonist) had positive lusitropic but no inotropic effect in EHT, and positive clinotropic, lusitropic, and inotropic effects in hAT. Tacrolimus (calcineurin-inhibitor) had a negative inotropic effect in EHTs, but no effect in hAT. Digoxin (Na^+-K^+-ATPase-inhibitor) showed a positive inotropic effect only in EHTs, but no effect in hAT probably due to short incubation time. Ryanodine (ryanodine receptor-inhibitor) reduced contraction force in both models. Rolipram and acetylsalicylic acid showed noninterpretable results in hAT. Contraction amplitude and kinetics were more stable over time and less variable in hiPSC-EHTs than hAT. HiPSC-EHT faithfully detected cAMP-dependent and -independent positive and negative inotropic effects, but limited beta-2 adrenergic or PDE3 effects, compatible with an immature CM phenotype.

Key words: blinded drug screening; safety pharmacology; cardiotoxicity; engineered heart tissue; iPS.

A major promise of human induced pluripotent stem cell-derived cardiomyocytes (hiPSC-CM) is to generate *in vitro* models with high predictivity. However, the stakes to reach this goal are high and require test systems with low variability and precise replication of drug effects. Different test systems have been published for hiPSC-CM including measurement of impedance (Guo *et al.*, 2011; Scott *et al.*, 2014), field potentials (FP) (Braam *et al.*, 2010; Caspi *et al.*, 2009; Harris *et al.*, 2013;

Navarrete et al., 2013), calcium and voltage measurements (Hwang et al., 2015; Lee et al., 2012; Lopez-Izquierdo et al., 2014), single cell shortening (Pointon et al., 2015) and electrophysiology (Hoekstra et al., 2012). Given the well-known differences between blinded and nonblinded analysis (MacCoun and Perlmutter, 2015), the validity of these test systems is probably best evaluated by blinded interlaboratory experiments. In a blinded single center study on FP in hiPSC-CM 9 out of 11 compounds revealed the expected effects, while two compounds, both I_{Ks} inhibitors, did not. FP prolongation by these two compounds was detectable in a second screen with attenuated repolarization reserve (Braam et al., 2013). Another study on hiPSC-CM was unable to distinguish between torsadogenic and benign compounds on the basis of FP duration and early afterdepolarization. The Na^+ slope was unable to differentiate between Na^+ channel and hERG blockade, beat rate was an inconsistent parameter, and the system was insensitive to I_{Ks} inhibitors (Qu and Vargas, 2015). Latest publications on a Comprehensive *in Vitro* Proarrhythmia Assay (CiPA) under blinded conditions showed platform and cell line-dependent differences, but overall high potential of hiPSC-CM for these applications (Blinova et al., 2017), whereas others report limited potential for detecting proarrhythmic drug effects with hiPSC-CM (Abi-Gerges et al., 2017) and cell line/batch-to-batch differences (Huo et al., 2016).

We have recently developed a contractility test system for hiPSC-CMs in engineered heart tissue (EHT) format based on video-optical recording. Proof-of-principle studies under nonblinded conditions indicated that a variety of drug effects including effects on inotropy, lusitropy, clinotropy, and chronotropy are replicated in hiPSC-EHTs (Mannhardt et al., 2016). We therefore set out to test the hypothesis that drug effects on contractile force and kinetics can also be demonstrated under blinded conditions in hiPSC-EHTs and compared the results to measurements in human atrial trabeculae (hAT) as a readily available state of the art reference.

MATERIALS AND METHODS

Blinded compound preparation. Powder aliquots of 10 compounds (milrinone, rolipram, citalopram, nifedipine, lidocaine, formoterol, tacrolimus, digoxin, acetylsalicylic acid, ryanodine) were prepared and labeled "1–10" at Novartis, Switzerland. Compounds, information on reconstitution in DMSO and working concentration were shipped to the UKE in Hamburg, Germany (4 °C, overnight express), where the experiments were performed. Experimentators were blinded for experimentation and data analysis and were only unblinded after data analysis had been completed.

Generation of hiPSC-EHTs. HiPSC-EHTs were prepared as recently described (Mannhardt et al., 2016). In brief, aliquots of iCell cardiomyocytes were thawed according to instruction manual and cardiomyocytes were counted automatically (CASY). HiPSC-EHT reconstitution mix was prepared with 1.0×10^6 cardiomyocytes per 100 µl hiPSC-EHT. EHTs were generated in agarose casting molds with solid silicone racks as previously described (Schaaf et al., 2014; Hansen et al., 2010). Briefly, casting molds were generated with agarose (2% in PBS; Invitrogen, 15510-019) and polytetrafluorethylene spacer (EHT Technologies, C0002) in 24-well plates (Nunc, 122475). Silicone racks (EHT Technologies, C0001) were placed on the 24-well plates. Cells (final concentration: 10×10^6 cells/ml) were mixed with 100 µl/ml Matrigel (BD Bioscience, 256235), 5 mg/ml bovine fibrinogen (Sigma, F4753; 200 mg/ml in 0.9% NaCl plus 0.5 µg/mg aprotinin; Sigma, A1153), 2 × DMEM (matching the volume of fibrinogen and thrombin for isotonization) and EHTs were generated with 100 µl per EHT (1.0×10^6 cells), 10 µM Y-27632 (Biorbyt, orb6014) and 3 U/ml thrombin (100 U/ml; Biopur, BP11101104). The cell mix was pipetted into agarose casting molds around the silicone posts. After fibrin polymerization (37 °C, 2 h) the silicone racks with attached fibrin gels were transferred to new 24-well plates filled with EHT medium (DMEM, 1% penicillin/streptomycin, 10% horse serum [Gibco, 26050], 10 µg/ml insulin [Sigma, I9278], 33 µg/ml aprotinin) and maintained in the incubator (37 °C, 40% O_2, 7% CO_2). Culture medium was changed Mondays, Wednesdays, and Fridays. After 10–14 days in culture human EHTs displayed spontaneous coherent contractions.

Analysis of contractile force. For EHT, force was measured based on automated video-optical recording and EHT contour recognition as recently described (EHT Technologies, A0001; Hansen et al., 2010). Human atrial trabeculae were analyzed in standard organ baths with mechanical force transducers.

Quality control. For hiPSC-EHTs, two characteristics were defined as quality control check points for this study: (1) the baseline force development was required to be at least 0.1 mN at 1.8 mM Ca^{2+} (tested in all hiPSC-EHTs; Figure 1B). (2) The positive inotropic response to isoprenaline (100 nM) in modified Tyrode's solution with a calcium concentration at [EC_{50}] was required to be at least 15% (tested in 4 EHTs per batch; Figure 1E). For hAT, quality control check points were defined as (1) positive Frank–Starling mechanism, (2) no decrease in diastolic length during equilibration phase, (3) robust muscle contractions during initial 90 min equilibration phase (Figure 1G).

Calcium concentration–response-curve in hiPSC-EHT. HiPSC-EHTs were transferred to 24-well plates containing modified low Ca^{2+} Tyrode's solution (0.1 mM). Steady state force was determined after 30 min of incubation. HiPSC-EHTs were then transferred to different 24-well plates and the Ca^{2+} concentration was cumulatively increased in modified Tyrode's solution to construct a concentration–response-curve.

Drug concentration–response-curve in hiPSC-EHT. The work flow for compound analysis is illustrated in Figure 2B. Drug screening was performed when EHT development reached the plateau phase with stable contraction forces starting around day 12 (Figure 1F). It included a baseline recording of contractility in the absence ("spontaneous") and presence of electrical pacing. Measurements were all done in parallel at two Ca^{2+} concentrations (1.8 mM ["high"] and 1.0 mM [EC_{50}; "low"]). This was followed by a half-logarithmic cumulative concentration–response-curve (incubation time 20 min per step) in the presence of electrical pacing. Electrical pacing was performed with carbon pacing electrodes as recently described (Hirt et al., 2014; 1–2 Hz). At the end of the concentration–response-curve, contractile force was also analyzed at the highest drug concentration without electrical pacing to determine possible effects on spontaneous beating rate. After the analysis was finished, compounds were washed out (3 times in modified Tyrode's solution with 1.8 mM Ca^{2+} for 20 min) and EHTs were transferred back to standard culture medium. HiPSC-EHTs were subjected to 2–4 (mean 3.3) different compounds. Between the experiments, hiPSC-EHTs were maintained for at least 2 days in standard culture medium for recovery. The history of compound exposure was registered in each case (see Supplementary Table 1). All compounds were measured with two different batches of hiPSC-EHTs.

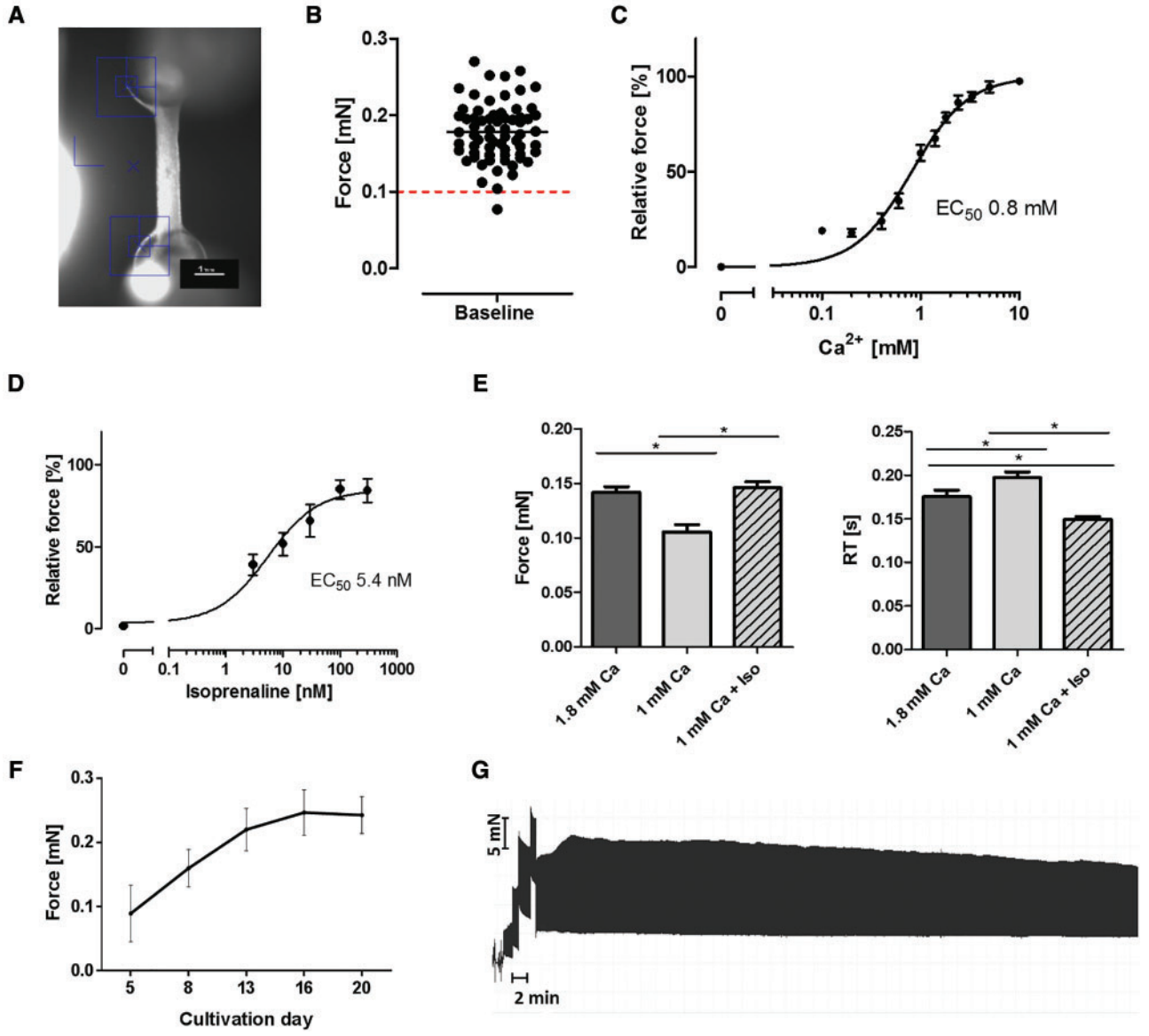

Figure 1. Quality control of hiPSC-EHTs and hAT in modified Tyrode's solution. A, Live image of a 12 days old EHT from hiPSC-CM. B, Baseline contraction force (1.8 mM Ca^{2+}) of spontaneously beating hiPSC-EHTs ($n = 66$) indicating the threshold value of 0.1 mN was reached for 65 hiPSC-EHTs. C, Calcium concentration–response-curve of hiPSC-EHTs (mean ± SEM; $n = 11$). D, Concentration–response-curve for isoprenaline (1 mM Ca^{2+}, 2 Hz; $n = 11$). E, Positive inotropic and lusitropic effect in response to isoprenaline indicated as changes in force and relaxation time (RT; 100 nM; one-way ANOVA, repeated measures, Bonferroni's post-test, $^*P < 0.05$; $n = 11$). F, Time course of EHT development depicting contraction force overtime indicating stable EHT contractility starting at day 20 (mean ± SD; $n = 12$). G, Exemplary original trace of a human atrial trabecula in the organ bath demonstrating Frank–Starling mechanism, stable diastolic tension and robust contractions over initial equilibration period of 90 min.

Drug concentration–response-curve in hAT. Human atrial trabeculae were obtained from the Department of Cardiac Surgery at the University Heart Centre Hamburg during elective surgical procedures. These studies were approved by the Medical Faculty Ethics Committee. All patients gave informed consent. Tissue samples were transported to the Department of Experimental Pharmacology and Toxicology and trabeculae isolated with scissors within 2 h. Human atrial trabeculae were subjected to blinded cumulative concentration–response-curves as previously described (Pecha *et al.*, 2015). In brief, hAT were mounted as pairs in an organ bath (37 °C, pH 7.4) in modified Tyrode's solution (1.8 mM Ca^{2+}) and stretched to resting tension giving half-maximum contraction force. After initial equilibration phase (90 min), a cumulative concentration–response-curve was initiated with 5 min incubation time per concentration step and electrical stimulation with 1 Hz. Two out of 8 hAT were kept as time-matched controls. Contraction data were recorded and analyzed with Chart 5.0 pro software (AD instruments). Contraction time (CT) and relaxation time (RT) were analyzed for 80% peak height.

Transcriptome analysis with the nanoString nCounter Elements TagSets. EHTs (30- to 36-day-old) were harvested, snap frozen in liquid nitrogen and stored at −80 °C. RNA was isolated from single or up to three pooled EHTs with RNeasy mini kit (Qiagen 74104) as previously published (Mannhardt *et al.*, 2016).

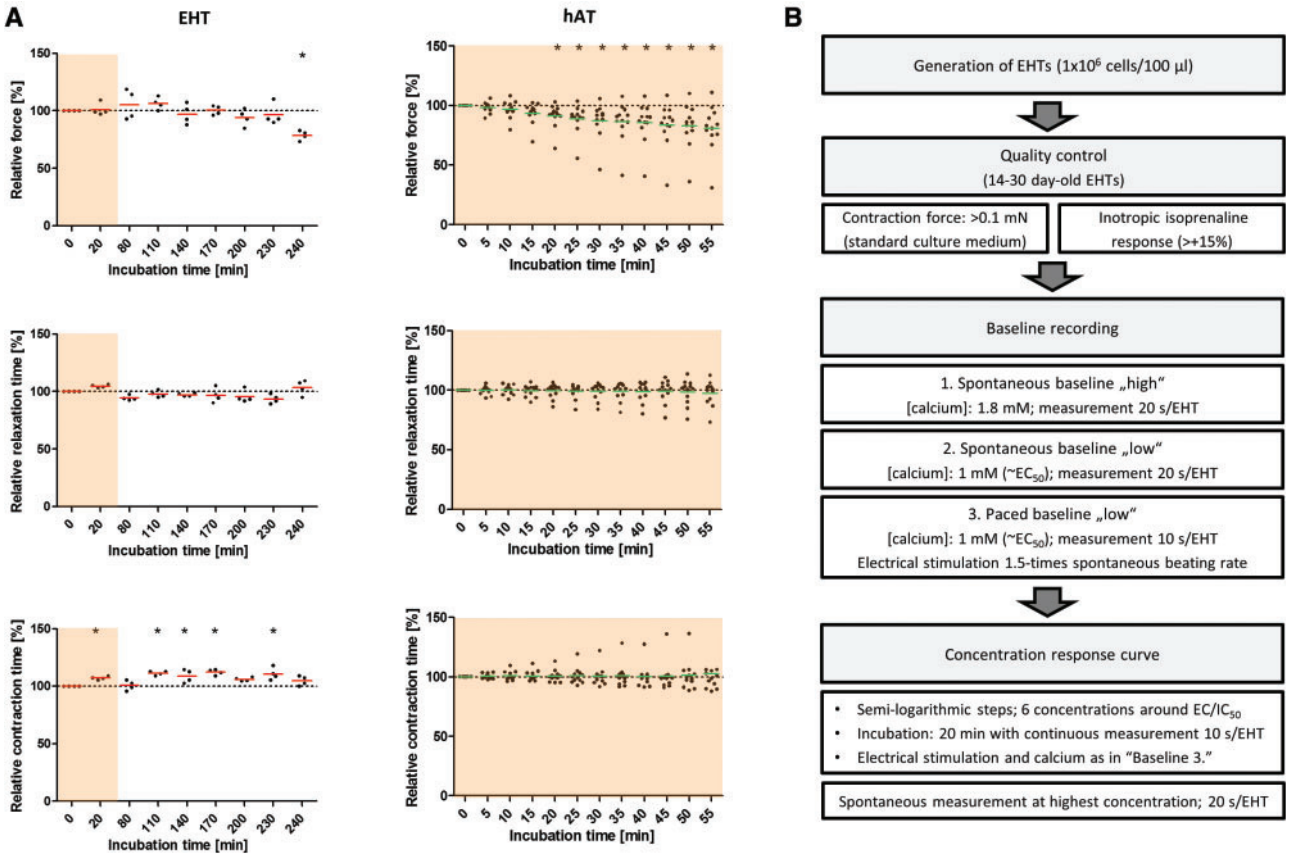

Figure 2. Drug screening standard operating procedure (SOP). A, Long-term stability of the test systems. Time control data for contraction force and kinetics during analysis of hiPSC-EHT (left panel; red) and hAT (right panel; green). Please note that total incubation time varies between hiPSC-EHT (up to 240 min) and hAT (up to 30 min) with the same time window of 55 min highlighted in color. Repeated measures ANOVA with Dunnett's post-test versus BL; *$P < 0.05$. B, Flow chart diagram of the SOP for cardiac drug screening on hiPSC-EHT.

Nonfailing human heart tissue not suitable for transplantation was obtained from University Heart Center with approval of the local ethical board and snap frozen at −80 °C. The heart tissue was pulverized with a cold steel mortar, homogenized with a TissueLyzer (Qiagen) and RNA isolated with the RNeasy kit. RNA concentration was determined per fluorometric quantitation with QubitTM according to the manufacturer's instructions. For transcriptome analysis, we designed a NanoString's nCounter Elements TagSet panel of 57 genes coding for proteins involved in excitation–contraction coupling or dysregulated in heart failure. Fifty nanograms of RNA per sample were hybridized to target-specific capture and reporter probes at 67 °C over night (16 h) according to the manufacturer's instructions. Samples were cooled down at 4 °C, loaded into the NanoString cartridge and nCounter Gene Expression Assay started immediately. Raw data (see Supplementary Table 2) were analyzed with nSolverTM Data Analysis Software including background subtraction using negative controls and normalization to 5 housekeeping genes (*ABCF1*, *CLTC*, *GAPDH*, *PGK1*, *TUBB*).

Statistics. Statistical analysis was performed with GraphPad Prism 5.0 software. Data in graphs are depicted as scatter plot with mean or mean ± SEM. Statistical tests were performed as indicated in the respective figure legend. Data in the text represent mean ± SD or mean only. Drug effects were considered relevant, if the ANOVA revealed a *P* value of less than .05 and the deviation from baseline was ≥15%. This threshold was defined after determination of variation coefficient of hiPSC-EHT force at baseline conditions (17 ± 5%; see results section on batch-to-batch variability) and previous studies on rat EHT (Eder *et al.*, 2014).

RESULTS

Quality Control

A total of 66 EHTs with 1× 10^6 cardiomyocytes/EHT were prepared and subjected to video-optical contractility recording for this study (Figure 1A). By quality control 1 hiPSC-EHT (1.5%) was excluded due to weak contraction forces below 0.1 mN at 1.8 mM Ca^{2+} when beating spontaneously (Figure 1B). Calcium concentration–response-curves revealed an EC_{50} of 0.8 mM Ca^{2+} (Figure 1C). An additional subset of hiPSC-EHTs was subjected to the second quality control step (inotropic response to 100 nM isoprenaline, 20-fold [EC_{50}], Figure 1D). The average positive inotropic effect amounted to +39% (from 0.11 ± 0.02 mN to 0.15 ± 0.02 mN) and the positive lusitropic effect to −25% (from 0.20 ± 0.02 s to 0.15 ± 0.01 s; $n = 12$; Figure 1E). All tested EHTs showed >15% increase in contraction force. From 88 hAT, one batch with 8 tissues was discarded due to spontaneous increase in diastolic tension during equilibration phase. The remaining 80 hAT were reduced by 10 (6 hAT with irregular beating at baseline, one with unstable contraction amplitudes during equilibration phase and three did not show an increase in force

upon stretching (data not shown). Overall, contraction measurements with hiPSC-EHTs showed higher level of robustness as compared to hAT. First significant time-dependent changes in time control hiPSC-EHTs were observed after 240 min, whereas the run-down in hAT was apparent after 20 min already (Figure 2A).

Variability

HiPSC-EHTs were prepared from 5 batches of iCell cardiomyocytes (different Lot numbers; batches 3–5 were used for this study). Overall variability of baseline parameters was smaller for hiPSC-EHT than for hAT. Values for hAT amounted to: Force 6.2 ± 3.5 mN, CT 0.08 ± 0.03 s, RT 0.11 ± 0.03 s; $n = 52$ hAT; Figure 3A). Values of hiPSC-EHT amounted to: Frequency 59 ± 12 bpm; force 0.18 ± 0.04 mN; CT 0.17 ± 0.03 s; RT 0.26 ± 0.04 s; $n = 107$ EHT; Figure 3B). Though lower than in hAT, the variability in EHTs was higher than expected, leading us to analyze individual batches of hiPSC-CM and therefore EHT. hiPSC-CM batch 5 was thawed in three independent EHT experiments (batch 5a, 5b, and 5c). The very low variability between the three thawings indicated that the main variability was derived from input CM batches rather than from thawing or EHT generation (Figure 3C). This intra-batch variability of baseline parameters was smaller for hiPSC-EHT than for hAT. Mean coefficients of variation (CV) (SD/mean× 100) were 10 ± 3% for frequency, 17 ± 5% for force, 5 ± 1% for CT, and 7 ± 1% for RT in hiPSC-EHT ($n = 8$ batches) and 49 ± 11% for force, 14 ± 11% for CT, and 21 ± 13% for RT ($n = 10$ batches) for hAT. Overall and intra-batch variabilities at baseline are listed in Table 1. To account for the variability at baseline, we analyzed drug effects compared to the respective baseline.

Drug Effects in hiPSC-EHTs and hAT

Drug effects in hiPSC-EHTs were determined at low (1 mM) and high (1.8 mM) Ca^{2+} according to the SOP depicted in Figure 2B. Results are demonstrated only for the data with 1.0 mM Ca^{2+}, as results in 1.8 mM Ca^{2+} Tyrode's solution were similar but less pronounced (data not shown). Drug effects in hAT were determined at 1.8 mM Ca^{2+}. Average contraction peaks for all 10 compounds versus baseline are demonstrated in Figure 4. Supplementary Figures 1 and 2 show complete concentrations-response-curves for force, CT and RT for hiPSC-EHT and hAT, respectively. Table 2 lists the effects for all compounds for hiPSC-EHT and hAT. In this table, small effects of less than 15% were not considered relevant (see Materials and Methods section on statistics). Coefficients of variation of 30 drug responses (force, CT, RT for 10 drugs) were lower in hiPSC-EHT than in hAT in 21/30 cases. For hiPSC-EHTs, both series of experiments are shown separately with compound history in each case (Supplementary Table 1).

The predominant PDE3A inhibitor (and less potent PDE4 inhibitor) milrinone (Bethke *et al.*, 1992) led to a positive inotropic (+97%) and lusitropic (RT: −22%) response in hAT, but did not have a significant effect on hiPSC-EHTs. The PDE4D inhibitor rolipram showed an unexpected constant-rate decline in contractile force in hAT, which was also apparent in the respective time-matched control hAT (contraction force declined to 67% of baseline; data not shown) and should therefore not be interpreted as a drug effect. In line with this assumption, no lusitropic or clinotropic effect was detected in the hAT. In contrast, hiPSC-EHTs demonstrated a positive lusitropic (RT: −23%) response to rolipram with no inotropic effect (Supplementary Figure 1), but an increase in spontaneous beating rate at 30 μM (+21%; paired Student's *t*-test $P < .0001$; $n = 8$; data not shown). The selective serotonin reuptake inhibitor (SSRI) citalopram reduced force in both hAT and hiPSC-EHT by 38% and 57%, respectively. The L-type calcium channel blocker nifedipine abolished force in hAT and hiPSC-EHT, albeit with different potency. The maximal effect was reached at 30 μM (hAT) and 0.3 μM (EHT), respectively. The sodium channel inhibitor lidocaine led to a negative inotropic effect in hAT (−36%) and hiPSC-EHT (−25%) with higher potency in hAT. The beta-2 adrenoceptor agonist formoterol led to a positive inotropic (+45%), clinotropic (CT: −40%) and lusitropic (RT: −19%) effect in hAT, whereas only a positive lusitropic effect (RT: −16%) could be detected in hiPSC-EHT. The calcineurin inhibitor tacrolimus did not affect hAT, but decreased force in hiPSC-EHT (−46%) with an additional negative clinotropic effect (CT: +20%). The cardiac glycoside digoxin did not show a positive inotropic effect in hAT (at the expected effective concentration of 0.3 μM), but a negative inotropic effect at higher concentrations. The latter can be interpreted as the well-known toxicity of higher concentration of cardiac glycosides. In hiPSC-EHT, both positive (+24%, 0.3 μM) and toxic negative inotropic effects (>1 μM) were detected. In addition, hiPSC-EHT showed a negative lusitropic effect (RT: −20%). Acetylsalicylic acid showed a constant-rate decline in contractile force in hAT that was not observed in the respective control hAT (data not shown). In hiPSC-EHT a small positive lusitropic effect (RT: −16%) was detected. The inhibitor of cardiac ryanodine receptors ryanodine reduced contractile force in hAT (−78% at 10 μM; −67% at 30 μM) and hiPSC-EHT (−33% at 0.1 μM; −21% at 30 μM) in a biphasic manner. This was accompanied by a strong negative lusitropic effect (RT: +84%) without change in CT in hAT and a strong negative clinotropic (CT: +60%) and positive lusitropic (RT: −21%) effect in hiPSC-EHT.

Carry-over Effects

Single hiPSC-EHTs were used to analyze effects of 2–4 different compounds with washout periods between measurements as indicated in Supplementary Table 1. To analyze if the differences in compound history also had an impact on drug effects, color-coded drug effects as listed in Table 2 (increase: green; decrease: red) were extended to the two series of hiPSC-EHT contractility results (Supplementary Table 1). It shows that most effects of the combined series were qualitatively similar in both series, but the size of the effect was substantially different between the two series in some cases (eg, citalopram, nifedipine, digoxin).

Transcriptome Analysis

Transcriptome analysis of three batches of iCell cardiomyocytes revealed slight batch-to-batch differences in gene expression, whereas variability between single or pooled EHTs of the same batch was minor (Figure 3D). The expression of 20 genes differed by >0.5 log units between batches (eg, *CASQ2, NPPB, ATP1A2, KCNJ2, KCNIP2*), but only 1 between samples of the same batch (*VWF*). Overall, gene expression in hiPSC-EHTs was quite similar to human nonfailing heart with notable exceptions such as >10-fold stronger expression of *NPPA, MYH6, HCN4, KCNJ5*, and much weaker expression of *MYH7, CASQ2, RCAN1, KNIP2*, and nonmyocyte markers such as *VWF, POSTN* (Supplementary Table 2).

DISCUSSION

The main findings of this blinded study on inotropic effects of 10 indicator compounds are as follows: (1) hiPSC-EHTs exhibited

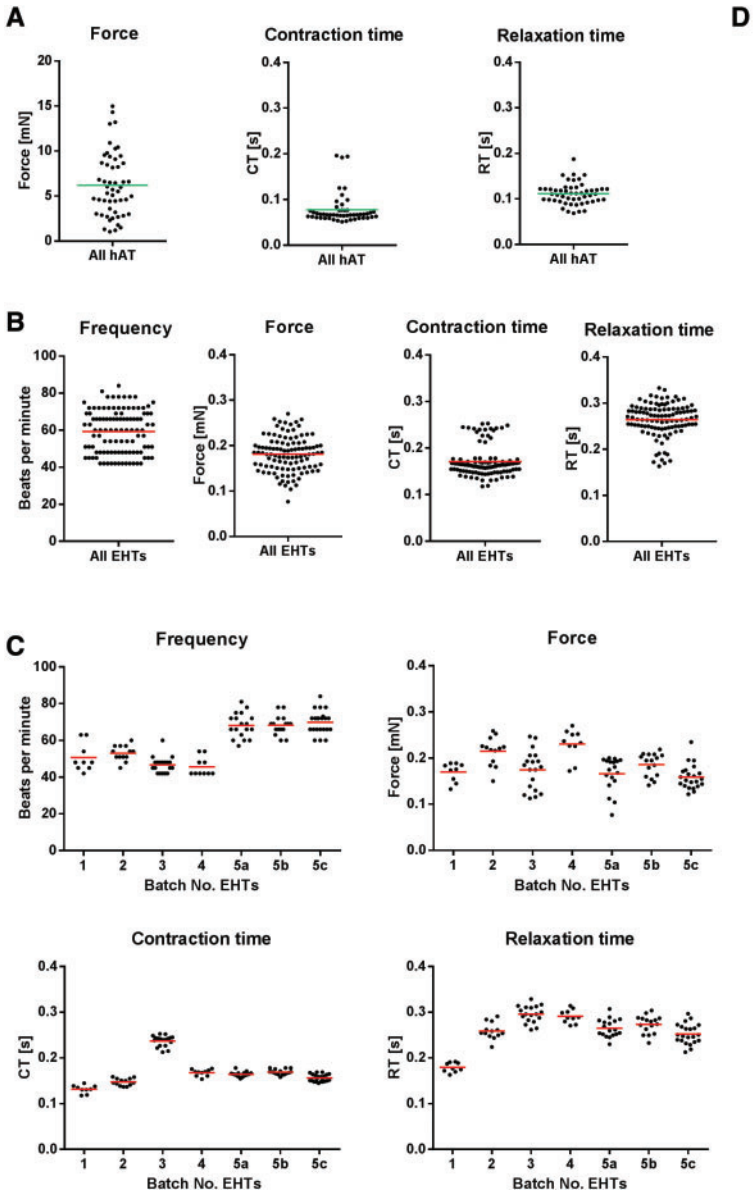

D

	NFH	hiPSC-EHT					
Gene	1	A	B1	B2	B3	C1	C2	C3
MYH7	5.4	4.7	4.7	4.8	4.7	4.6	4.6
PLN	4.8	4.8	4.9	4.9	4.9	4.8	4.8	4.8
SLC8A1	4.7	4.5	4.4	4.4	4.5	4.4	4.3	4.3
FHL1	4.6	3.3	3.3	3.3	3.3	3.1	2.9	3.0
ACTN2	4.5	4.4	4.2	4.2	4.3	4.2	4.1	4.2
RYR2	4.2	3.8	3.9	3.9	3.9	3.6	3.6	3.6
CASQ2	4.1	3.3	3.2	3.2	3.1	2.8	2.7	2.7
FHL2	3.8	4.3	4.2	4.2	4.3	4.3	4.2	4.3
ATP2A2	3.6	4.0	4.1	4.0	4.0	3.9	3.8	3.8
NPPA	3.6	5.1	4.7	4.7	4.8	5.0	4.9	4.9
RCAN1	3.6	3.2	2.7	2.7	2.9	2.8	2.8	2.7
ATP1A1	3.5	3.9	3.9	3.9	4.0	4.0	3.9	3.9
NPPB	3.4	3.5	3.2	3.2	3.1	3.7	3.9	3.8
S100A4	3.4	3.1	3.1	3.1	3.1	3.3	3.3	3.3
ATP1A2	3.4	2.8	2.5	2.5	2.4	2.3	2.3	2.3
VWF	3.3	1.0	0.6	0.0	0.0	0.0	0.0	0.4
POSTN	3.2	2.5	1.8	1.6	1.6	2.1	2.2	2.2
KCNJ2	3.1	2.7	2.7	2.7	2.9	2.0	2.0	2.0
FN1	3.1	2.1	2.0	1.8	1.9	2.6	2.5	2.6
COL3A1	3.1	2.1	2.3	2.1	2.1	2.8	2.7	2.8
PPP1R1A	3.0	3.5	3.7	3.7	3.6	3.6	3.5	3.6
CTGF	3.0	2.9	2.1	1.9	1.7	2.4	2.1	2.4
SRF	3.0	3.2	3.2	3.1	3.2	3.1	3.0	3.0
KCNIP2	3.0	1.5	1.2	1.0	1.1	0.7	0.7	0.7
CDH5	3.0	1.8	1.6	1.4	1.4	1.5	1.6	1.5
SCN5a	2.9	3.3	3.3	3.4	3.4	3.3	3.3	3.3
BCL2	2.8	2.0	1.5	1.4	1.6	1.4	1.2	1.0
CASP3	2.7	3.1	2.9	2.9	3.0	2.9	2.8	2.9
KCNQ1	2.7	2.9	2.9	2.8	3.0	2.9	2.8	2.8
KCNH2	2.7	3.0	2.9	2.9	2.8	2.8	2.8	2.9
CACNA1C	2.6	3.1	2.9	2.9	2.9	2.9	2.8	2.9
BAX	2.6	2.9	2.8	2.7	2.8	2.8	2.7	2.7
MYH6	2.5	4.7	4.6	4.5	4.5	4.6	4.4	4.5
COL1A1	2.5	2.1	2.2	2.1	2.1	2.2	2.1	2.2
KCND3	2.4	1.6	1.7	1.7	1.7	1.5	1.2	1.3
MEOX1	2.3	1.6	0.0	0.0	0.0	0.0	0.0	0.0
KCNJ11	2.3	2.0	2.1	2.1	2.1	1.7	1.8	1.7
KCNA4	2.2	2.7	2.9	2.8	2.8	2.4	2.3	2.4
KCNA5	2.1	2.1	1.6	1.5	1.6	1.5	1.5	1.6
KCNE1	2.1	1.8	1.5	1.5	1.5	1.3	1.4	1.6
SLC9A1	2.0	2.3	2.3	2.3	2.2	2.2	2.1	2.1
NFKB1	2.0	2.0	1.8	1.7	1.7	1.4	1.4	1.3
KCNJ5	1.9	2.8	3.0	3.0	3.0	2.9	2.8	2.9
KCNJ12	1.7	1.3	1.3	1.1	1.4	1.4	1.5	1.5
KCNN3	1.5	1.9	1.8	1.8	1.7	1.6	1.6	1.7
CACNA1G	1.5	3.0	2.9	2.9	2.8	2.8	2.7	2.8
HCN4	1.3	2.8	2.7	2.7	2.6	2.5	2.4	2.5
KCNE2	1.0	1.6	1.5	1.5	1.6	1.4	1.4	1.5
KCNJ3	1.0	2.3	2.3	2.1	2.1	1.8	1.7	1.8
SCN10A	1.0	1.9	1.2	1.2	1.1	1.4	1.4	1.4

High
Low

Figure 3. Batch-to-batch variability. Contractile parameter of electrically stimulated hAT (A) and spontaneously beating hiPSC-EHTs (B, C). A, Human atrial trabeculae from 10 different patients electrically stimulated with 1 Hz ($n = 52$). B, HiPSC-EHTs from 5 different batches at days 12–22 post casting ($n = 107$). C, EHT contractility data divided by batch number ($n = 9$-19 per batch). Batch 5a–5c indicate three independent thawings and hiPSC-EHT generation from the same batch of cells. Note the larger scatter of contraction force in the hAT (A) versus hiPSC-EHT (B). See also Table 1. D, Transcriptome analysis of human nonfailing heart (NFH) and 3 batches (A–C) of hiPSC-CM in EHT-format showing heat map of gene expression normalized to housekeeping genes. Gene expression is expressed as log 10 values and color coded with high expression levels marked in green and low gene expression levels red. Batch B is split into three single EHTs of the same batch (B1, B2, B3) and batch C is split into three pools of 2–3 EHTs each (C1, C2, C3). Grey highlighted genes show significant variability in gene expression ($\geq \log_{10} 0.5 \approx 3$-fold) between the three hiPSC cell batches. See also Supplementary Table 2 for raw data and abbreviations of gene names.

less baseline variability than hAT, with mean variation coefficients of force development amounting to 17% versus 49%. Force development of hiPSC-EHTs demonstrated considerably higher stability over time, allowing medium-to-long-term measurements. (2) hiPSC-EHTs showed the expected drug effects on contractile force for citalopram, lidocaine, nifedipine ryanodine, acetylsalicylic acid, as well as isoprenaline, used as positive control. Data on tacrolimus are inconsistent in literature and showed different effects in hiPSC-EHT and hAT. (3) PDE4 appears to be the major PDE isoform controlling contractile function in hiPSC, while PDE3 dominates in hAT. (4) hiPSC-EHTs did not show positive inotropic effect upon beta-2 adrenergic stimulation with formoterol. (5) Overall, the positive inotropic effects of cAMP-dependent drugs were smaller in hiPSC-EHTs than in hAT, indicative of an immature beta-adrenergic/cAMP system.

Compound 1: Milrinone (0.1-30 μM), Compound 2: Rolipram (0.1-30 μM)

Selective inhibition of PDE 3 by cilostamide leads to a small positive inotropic and lusitropic response in human atrial (Christ *et al.*, 2006) but not ventricular (Molenaar *et al.*, 2013) tissue, while PDE4 inhibition (rolipram) did not modify force in either tissue (Berk *et al.*, 2016; Molenaar *et al.*, 2013). These findings

Table 1. Baseline Contractility Data of hiPSC-EHT and hAT for Contractile Force, Contraction Time CT and Relaxation Time RT

	Force	CT	RT
HiPSC-EHT			
Mean ± SD (n=107)	0.18 ± 0.04 mN	0.17 ± 0.03 s	0.26 ± 0.04 s
Overall CV (n=107 EHTs)	CV = 22%	CV = 18%	CV = 15%
Mean Intra-batch CV (n=5 batches of EHT)	17%	5%	7%
Human atria			
Mean ± SD (n = 52)	6.2 ± 3.5 Mn	0.08 ± 0.03 s	0.11 ± 0.02 s
Overall CV (n = 52 hAT)	56%	38%	18%
Mean Intra-batch CV (n = 10 batches of hAT)	49%	14%	21%

Depicted are absolute values as mean ± SD for force, CT and RT as well as coefficients of variation (CV) quantifying overall and intra-batch variability.

align well with milrinone effects in hAT. The negative inotropic effect observed in hAT with rolipram is explained by larger run-down in this particular batch of tissues as the variability in time control was large in hAT and the respective time control hAT showed a decrease in force of up to 67%. The positive lusitropic and positive chronotropic effect of rolipram in hiPSC-EHT conforms to the mode of action of PDE inhibitors. The predominance of PDE4 over PDE3 is likely an indicator for cardiomyocyte immaturity since it was shown that the switch from PDE4 to PDE3 occurs postnatally in rabbit and pig heart development (Akita *et al.*, 1994; Galindo-Tovar *et al.*, 2010).

Compound 3: Citalopram (0.1–30 μM), Compound 4: Nifedipine (0.1–30 μM)

The negative inotropic effect of citalopram is likely independent of the primary mechanism of action (SSRI) and in line with a published report in isolated guinea-pig atria suggesting that citalopram mediates A1 adenosine receptor agonistic effect (Pousti *et al.*, 2004). The potency (IC_{50}: 10 μM) suggests that this effect is not relevant under normal antidepressant treatment (plasma concentration 300 nM; Gutierrez and Abramowitz, 2000). L-Type calcium channel block by nifedipine leads to a strong negative inotropic effect and reversible cease of beating (Brixius *et al.*, 2005). In both models a strong negative inotropic effect was seen, but at different concentrations (maximal effect in hAT: 30 μM, hiPSC-EHT: 0.3 μM). This difference in sensitivity is in line with the unusually high sensitivity of hiPSC-CM/EHTs to external Ca^{2+} (EC_{50}: 0.8 mM versus ~3 mM in hAT). On the other hand, the values for hiPSC-EHTs conform better with a previous report in hAT reporting a maximal effect at 1 μM (Brixius *et al.*, 2005). The short incubation time in the organ bath measurement and the light sensitivity of the compound though, might have contributed to the discrepancy in results. The dramatic decreases in contraction force in hiPSC-EHT after exposure to citalopram and nifedipine also led to decreased kinetics (CT, RT).

Compound 5: Lidocaine (0.1–30 μM)

Lidocaine reduces force, but the underlying mechanism is not entirely clear (Pankucsi *et al.*, 1996; Schlepper, 1989). The negative inotropic effect seen in both models in this study is in line with literature data on dog and rat (David *et al.*, 2007; Tsuboi and Chiba, 1999). While less selective sodium channel inhibitors (quinidine, procainamide) also interact with hERG channels and lead to prolongation in RT, this is not expected for lidocaine. Highly selective blockers such as tetrodotoxin did not affect contractile force, nor RT in hiPSC-EHTs (Mannhardt *et al.*, 2016).

Compound 6: Formoterol (0.01–3.0 μM)

A specific feature of adult human myocardium (in contrast to rodent) is the relevant contribution of beta-2 adrenoceptors to the beta-adrenergic positive inotropic effect of nonselective agonists (Molenaar *et al.*, 2000). Formoterol increased force by 45% in hAT in the present study with similar potency to previously published studies in guinea pig (Lemoine and Overlack, 1992), but had no significant effect on force in hiPSC-EHTs. It did also show a positive lusitropic (RT) and clinotropic (CT) effect in hAT, but only a small positive lusitropic effect in hiPSC-EHTs. In hiPSC-CM models isoprenaline was frequently used and was reported to lead to small effects across different models (effect size: < +100%; Denning *et al.*, 2016) compared to human nonfailing heart tissue (effect sizes more than 200%; Bohm *et al.*, 1991; Mügge *et al.*, 1985; Schotten *et al.*, 2001), suggesting that cAMP/PKA signaling is functional, but small in hiPSC-CM. A more detailed analysis of the effect of culture time on beta-adrenoceptor expression showed that beta-2 expression dropped within 90 days (Jung *et al.*, 2016). Both beta-adrenoceptors were shown to be functionally coupled to cAMP/PKA signaling pathway. On the other hand, in the same study, beta-2, but not beta-1 adrenoceptors rapidly desensitized in response to agonist exposure by β-arrestin/clathrin-mediated endocytosis (Jung *et al.*, 2016). Such a mechanism would attenuate a formoterol effect and could explain the lack of effect shown in this study.

Compound 7: Tacrolimus (0.1–30 μM)

The calcineurin inhibitor tacrolimus binds to FKBP 12.6 and might modulate SR calcium release in cardiomyocytes. Furthermore, it inhibits hERG (−30% at 10 μM; Kise *et al.*, 2009) and reduces L-type calcium currents (25 μM; Fauconnier *et al.*, 2005). The reported effects on heart tissue are inconsistent. While one study reported a positive inotropic effect in rat cardiomyocytes (5 μM; McCall *et al.*, 1996), another study did not find any effect on force in human (10 nM to 10 μM) and a small positive inotropic effect in rabbit atrial trabeculae (10 μM; Milting *et al.*, 2001). In contrast, tacrolimus exerted negative inotropic effects (0.1 mg/kg body weight) in a model of anesthetized dogs (Kise *et al.*, 2009). We observed a clear negative inotropic effect at 10 μM associated with prolonged CT and a tendency for a biphasic effect on RT (see Supplementary Figure 1) in hiPSC-EHTs, but no effect on hAT. Given the incomplete understanding of the tacrolimus effect on heart muscle contractility, it is difficult to categorize the findings obtained in this study. Nevertheless, the negative inotropic effect and the prolongation of relaxation are compatible with inhibition of L-type calcium and hERG channels, while the prolongation of CT is compatible with an inhibitory effect on ryanodine receptors (see also ryanodine). Given the therapeutic plasma concentration in the low nanomolar range (Tremblay *et al.*, 2016) though, the effects observed in this study are most likely not clinically relevant.

Compound 8: Digoxin (0.1–30 μM)

Sodium-potassium ATPase inhibitors indirectly increase cytosolic calcium concentrations and, in isometrically contracting heart tissue preparations, cause a harmonic increase in

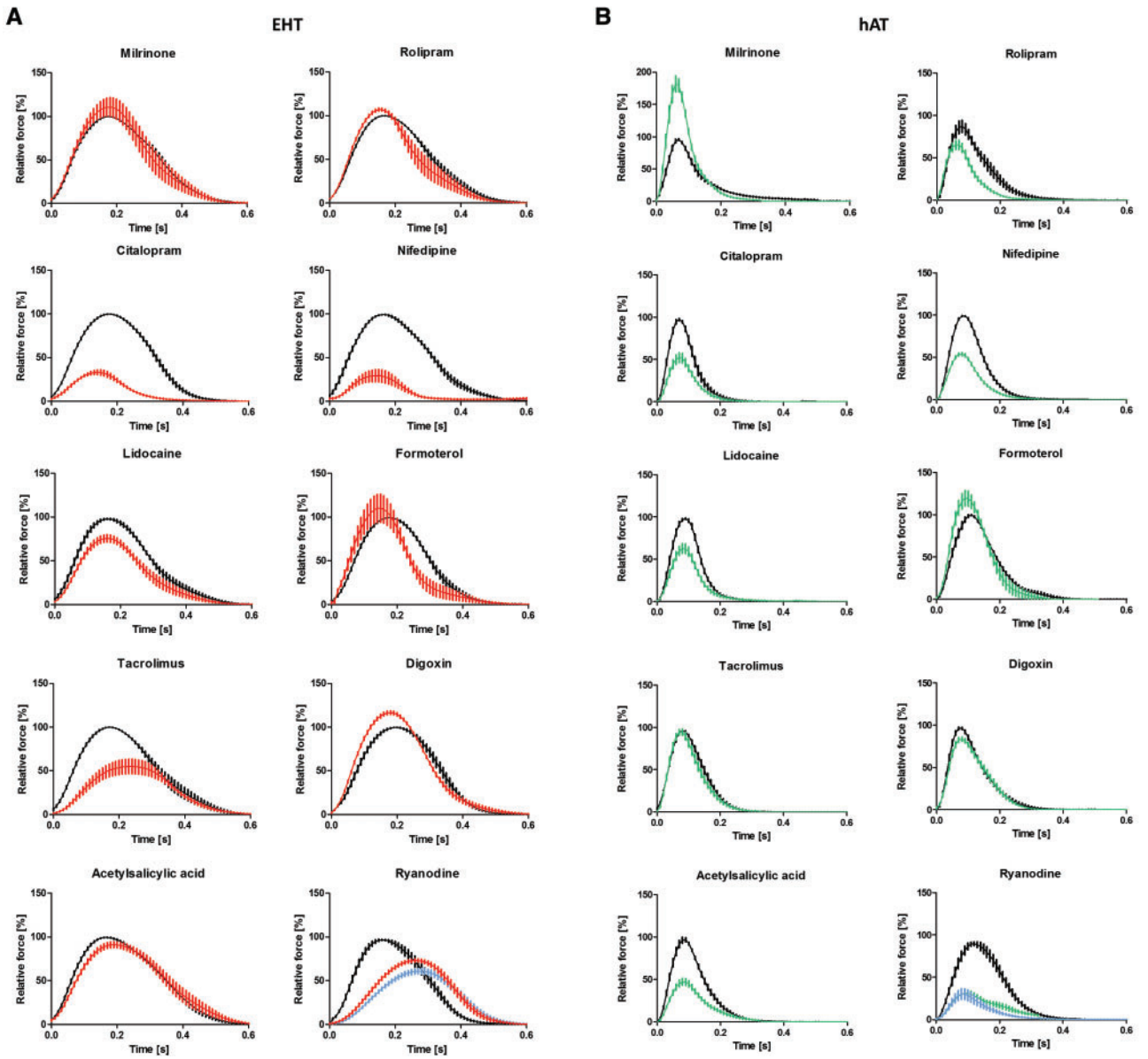

Figure 4. Blinded drug screening of 10 compounds. Average contraction peaks. A, Average contraction peaks of electrically stimulated hiPSC-EHTs in modified Tyrode's solution (1.0 mM Ca^{2+}) indicating relative force normalized to baseline over time. Four to eight EHTs per average peak. Black: baseline. Red: compound at indicated concentration (30 μM milrinone, 30 μM rolipram, 10 μM citalopram, 0.1 μM nifedipine, 30 μM lidocaine, 0.3 μM formoterol, 30 μM tacrolimus, 0.3 μM digoxin, 30 μM acetylsalicylic acid, 30 μM, and 0.3 μM [blue] ryanodine). B, Average contraction peaks of electrically stimulated hAT in modified Tyrode's solution (1.8 mM Ca^{2+}). Four to six hAT per average peak. Black: baseline. Green: compound at indicated concentration (30 μM milrinone, 30 μM rolipram, 10 μM citalopram, 3 μM nifedipine, 30 μM lidocaine, 3 μM formoterol, 30 μM tacrolimus, 3 μM digoxin, 30 μM acetylsalicylic acid, 30 μM, and 3 μM [blue] ryanodine). Please note the different ordinate scale in the milrinone graph of the hAT measurement and the different concentrations of nifedipine, formoterol and digoxin in hiPSC-EHT versus hAT.

contractile force (Reiter, 1972). The results obtained with hiPSC-EHT conform to the reported inotropic effects. The lack of positive inotropic effect in hAT is very likely due to the short incubation times of only 5 min per concentration and the slow kinetic of this effect (Kuschinsky *et al.*, 1967; Lüllmann and Ravens, 1973). The therapeutic window of digoxin is small and higher concentrations are toxic and lead to cease of beating which could be observed in both hiPSC-EHT and hAT.

Compound 9: Acetylsalicylic Acid (0.1–30 μM)

Acetylsalicylic acid has no effects on cardiac excitation–contraction coupling and was expected not to change force or kinetics of contraction as shown previously in a hiPSC-EHT study based on a different cell line (Mannhardt *et al.*, 2016). In the present study, a small positive lusitropic effect was observed in hiPSC-EHT and a constant decline in contraction force in hAT. The relevance of these findings is not clear and would require further investigation. The high level of force rundown in hAT was not found in the respective time control hAT in the acetylsalicylic acid experiment. But due to the high variability between hAT, rundown phenomena and/or poor hAT quality could only be excluded with increased replicate numbers.

Compound 10: Ryanodine (0.1–30 μM)

Ryanodine has complex actions on cardiac ryanodine receptors (RyR2) controlling the sarcoplasmic reticulum Ca^{2+} release. At

Table 2. Mean Values for Drug Effects on Contractile Force, Contraction Time (CT) and Relaxation Time (RT) in hiPSC-EHTs Versus Results in hAT

Compound	Mode of Action	Concentration (μM)	Parameter	Effect on hiPSC-EHTs (% of BL)	CV (%)	Effect on Human Atria (% of BL)	CV (%)
Milrinone	PDE3 inhibitor	30	Force	104	8	197	22
			CT	103	5	91	4
			RT	87	14	78	8
Rolipram	PDE4 inhibitor	30	Force	105	6	61	37
			CT	92	7	88	5
			RT	77	16	93	8
Citalopram	SSRI	30	Force	43	9	62	29
			CT	72	4	103	5
			RT	57	9	106	18
Nifedipine	LTCC blocker	0.1	Force	50	14	85	8
			CT	74	4	97	3
			RT	63	3	102	4
Lidocaine	Sodium channel blocker	30	Force	75	15	64	33
			CT	98	5	94	4
			RT	91	4	106	18
Formoterol	Beta 2 agonist	0.3	Force	110	13	145	20
			CT	94	15	60	23
			RT	84	7	81	14
Tacrolimus	Calcineurin inhibitor	30	Force	54	42	95	18
			CT	120	4	87	13
			RT	86	9	100	11
Digoxin	Sodium-potassium ATPase inhibitor	0.3	Force	124	7	92	8
			CT	94	7	99	10
			RT	80	14	100	3
Acetylsalicylic acid	COX inhibitor	30	Force	98	9	48	34
			CT	112	10	104	4
			RT	84	12	113	19
Ryanodine	Ryanodine receptor inhibitor	30	Force	80	16	33	23
			CT	160	13	94	32
			RT	79	7	184	26

Listed are mean effects on hiPSC-EHTs or human atrial preparations in percent of baseline (% of BL) at the indicated concentration and the respective coefficient of variation (CV). Color coding marks significant and relevant (≥15% effect) increase (green) and decrease (red).

low (nanomolar) concentrations, it sensitizes the channel to Ca^{2+} and promotes RyR2 opening, in higher concentration it inhibits its open probability (Cheng *et al.*, 1993). The effect on human heart tissue contractile force is poorly described. We observed a strong negative inotropic effect in both preparations in this study, but different effects on contraction kinetics. A negative clinotropic effect in hiPSC-EHTs was accompanied by a positive lusitropic effect, while ryanodine did not affect CT and prolonged RT in hAT. A study on cardiac preparations from rat, dog, rabbit and cat (Sutko and Willerson, 1980) suggested that negative inotropy and clinotropy is a common consequence of ryanodine, but at different magnitude. A more detailed analysis on cat papillary muscles described biphasic effects on contraction with early positive and delayed negative lusitropic effects, very similar to our observations in hiPSC-EHTs (Sutko *et al.*, 1979). Given ryanodine's complex mode of action and the poor characterization of ryanodine effects on human heart tissue, the findings of this study are compatible with literature data and data from previous EHT studies (Mannhardt *et al.*, 2016), but details remain unclear.

Force Run-Down and Relevance Threshold

Run-down in contractile force of hAT and the variability between different time-matched control hAT over time (Figure 2A, 4% after 5 min versus 24% after 55 min) have to be considered when evaluating the data presented in this manuscript. This makes it very difficult to detect negative inotropic effects and requires high numbers of replicates. HiPSC-EHTs, on the other hand, demonstrated with no run-down and less variability. To discriminate small biological effects from variability, we (Eder *et al.*, 2014) and others (Crumb *et al.*, 2016) have therefore implemented a "relevance threshold". Based on this, only statistically significant changes of more than 15% should be considered relevant drug effects.

hAT versus hiPSC-EHTs

In comparison with hAT, the lack of beta-2 adrenergic effects, the dominance of PDE4 over PDE3 and the overall small size of the response to beta-adrenergic/cAMP dependent drugs in hiPSC-EHTs are limitations. The unphysiologically high sensitivity to calcium is notable and may be associated with the higher sensitivity to nifedipine. Disadvantages of hiPSC-EHT are balanced by advantages, ie, (1) smaller variability of basal force development and most drug responses, (2) lack of force run-down that impedes identification of negative inotropic effects in the hAT assay, (3) principally unlimited availability, (4) higher versatility (eg, possibility of genome editing by CRISPR/Cas9 technology, AAV transduction or the modulation of cellular composition), and (5) the ventricular phenotype of hiPSC-CM/EHTs compared to the atrial phenoytpe of hAT. While hiPSC-CM

seem to mature in the EHT format in some structural and functional parameters (Mannhardt *et al.*, 2016; Uzun *et al.*, 2016), further means to improve maturation are imperative to boost the predictive value of hiPSC-CM in drug testing.

CONCLUSION

This study demonstrates that hiPSC-EHT are feasible to detect inotropic effects of drugs with various modes of action under blinded conditions, but failed to detect beta-2 adrenergic or PDE3 effects.

SUPPLEMENTARY DATA

Supplementary data are available at *Toxicological Sciences* online.

FUNDING

The work of the authors is supported by grants from the DZHK (German Centre for Cardiovascular Research) and the German Ministry of Education and Research (BMBF), the German Research Foundation (DFG Es 88/12-1), British National Centre for the Replacement Refinement & Reduction of Animals in Research (NC3Rs CRACK-IT grant 35911-259146), the British Heart Foundation RM/13/30157, the EU (FP7 Biodesign), the European Research Council (ERC Advanced Grant IndivuHeart), the German Heart Foundation and the Freie und Hansestadt Hamburg as well as financial support from Novartis Institutes of Biomedical Research".

ACKNOWLEDGEMENTS

The authors thank Simon Pecha and the EHT group for their kind support and the members of the CRACK-IT consortium for fruitful discussion.

CONFLICT OF INTEREST

I.M., A.E., T.E., and A.H. are founders of EHT Technologies GmbH, Germany.

REFERENCES

Abi-Gerges, N., Pointon, A., Oldman, K. L., Brown, M. R., Pilling, M. A., Sefton, C. E., Garside, H., and Pollard, C. E. (2017). Assessment of extracellular field potential and Ca2+ transient signals for early QT/pro-arrhythmia detection using human induced pluripotent stem cell-derived cardiomyocytes. *J. Pharmacol. Toxicol. Methods* **83**, 1–15.

Akita, T., Joyner, R. W., Lu, C., Kumar, R., and Hartzell, H. C. (1994). Developmental changes in modulation of calcium currents of rabbit ventricular cells by phosphodiesterase inhibitors. *Circulation* **90**, 469–478.

Berk, E., Christ, T., Schwarz, S., Ravens, U., Knaut, M., and Kaumann, A. J. (2016). In permanent atrial fibrillation, PDE3 reduces force responses to 5-HT, but PDE3 and PDE4 do not cause the blunting of atrial arrhythmias. *Br. J. Pharmacol.* **173**, 2478–2489.

Bethke, T., Meyer, W., Schmitz, W., Scholz, H., Stein, B., Thomas, K., and Wenzlaff, H. (1992). Phosphodiesterase inhibition in ventricular cardiomyocytes from guinea-pig hearts. *Br. J. Pharmacol.* **107**, 127–133.

Blinova, K., Stohlman, J., Vicente, J., Chan, D., Johannesen, L., Hortigon-Vinagre, M. P., Zamora, V., Smith, G., Crumb, W. J., Pang, L., *et al.* (2017). Comprehensive translational assessment of human induced pluripotent stem cell derived cardiomyocytes for evaluating drug-induced arrhythmias. *Toxicol. Sci.* **155**, 234–247.

Bohm, M., Morano, I., Pieske, B., Ruegg, J. C., Wankerl, M., Zimmermann, R., and Erdmann, E. (1991). Contribution of cAMP-phosphodiesterase inhibition and sensitization of the contractile proteins for calcium to the inotropic effect of pimobendan in the failing human myocardium. *Circ. Res.* **68**, 689–701.

Braam, S. R., Tertoolen, L., Casini, S., Matsa, E., Lu, H. R., Teisman, A., Passier, R., Denning, C., Gallacher, D. J., Towart, R., *et al.* (2013). Repolarization reserve determines drug responses in human pluripotent stem cell derived cardiomyocytes. *Stem Cell Res.* **10**, 48–56.

Braam, S. R., Tertoolen, L., van de Stolpe, A., Meyer, T., Passier, R., and Mummery, C. L. (2010). Prediction of drug-induced cardiotoxicity using human embryonic stem cell-derived cardiomyocytes. *Stem Cell Res.* **4**, 107–116.

Brixius, K., Gross, T., Tossios, P., Geissler, H.-J., Mehlhorn, U., Schwinger, R. H. G., and Hekmat, K. (2005). Increased vascular selectivity and prolonged pharmacological efficacy of the L-type Ca2+ channel antagonist lercanidipine in human cardiovascular tissue. *Clin. Exp. Pharmacol. Physiol.* **32**, 708–713.

Caspi, O., Itzhaki, I., Kehat, I., Gepstein, A., Arbel, G., Huber, I., Satin, J., and Gepstein, L. (2009). In Vitro Electrophysiological Drug Testing Using Human Embryonic Stem Cell Derived Cardiomyocytes. *Stem Cells Dev.* **18**, 161–172.

Cheng, H., Lederer, W. J., and Cannell, M. B. (1993). Calcium sparks: Elementary events underlying excitation-contraction coupling in heart muscle. *Science* **262**, 740–744.

Christ, T., Engel, A., Ravens, U., and Kaumann, A. J. (2006). Cilostamide potentiates more the positive inotropic effects of (-)-adrenaline through ß2-adrenoceptors than the effects of (-)-noradrenaline through β1-adrenoceptors in human atrial myocardium. *Naunyn. Schmiedebergs. Arch. Pharmacol.* **374**, 249–253.

Crumb, W. J., Vicente, J., Johannesen, L., and Strauss, D. G. (2016). An evaluation of 30 clinical drugs against the comprehensive in vitro proarrhythmia assay (CiPA) proposed ion channel panel. *J. Pharmacol. Toxicol. Methods* **81**, 251–262.

David, J.-S., Amour, J., Duracher, C., Ferretti, C., Precloux, P., Petit, P., Riou, B., and Gueugniaud, P.-Y. (2007). Comparison of the effects of mepivacaine and lidocaine on rat myocardium. *Eur. J. Anaesthesiol.* **24**, 190–197.

Denning, C., Borgdorff, V., Crutchley, J., Firth, K. S. A., George, V., Kalra, S., Kondrashov, A., Hoang, M. D., Mosqueira, D., Patel, A., *et al.* (2016). Cardiomyocytes from human pluripotent stem cells: From laboratory curiosity to industrial biomedical platform. *Biochim. Biophys. Acta* **1863**, 1728–1748.

Eder, A., Hansen, A., Uebeler, J., Schulze, T., Neuber, C., Schaaf, S., Yuan, L., Christ, T., Vos, M. A., and Eschenhagen, T. (2014). Effects of proarrhythmic drugs on relaxation time and beating pattern in rat engineered heart tissue. *Basic Res. Cardiol.* **109**, 436.

Fauconnier, J., Lacampagne, A., Rauzier, J.-M., Fontanaud, P., Frapier, J.-M., Sejersted, O. M., Vassort, G., and Richard, S. (2005). Frequency-dependent and proarrhythmogenic effects of FK-506 in rat ventricular cells. *Am. J. Physiol. Heart Circ. Physiol.* **288**, H778–H786.

Galindo-Tovar, A., Vargas, M. L., and Kaumann, A. J. (2010). Function of cardiac beta1- and beta2-adrenoceptors of newborn piglets: Role of phosphodiesterases PDE3 and PDE4. *Eur. J. Pharmacol.* **638**, 99–107.

Guo, L., Abrams, R. M. C., Babiarz, J. E., Cohen, J. D., Kameoka, S., Sanders, M. J., Chiao, E., and Kolaja, K. L. (2011). Estimating the risk of drug-induced proarrhythmia using human induced pluripotent stem cell-derived cardiomyocytes. *Toxicol. Sci.* **123**, 281–289.

Gutierrez, M. M., and Abramowitz, W. (2000). Pharmacokinetic comparison of oral solution and tablet formulations of citalopram: A single-dose, randomized, crossover study. *Clin. Ther* **22**, 1525–1532.

Hansen, A., Eder, A., Bönstrup, M., Flato, M., Mewe, M., Schaaf, S., Aksehirlioglu, B., Schwoerer, A. P., Uebeler, J., and Eschenhagen, T. (2010). Development of a drug screening platform based on engineered heart tissue. *Circ. Res.* **107**, 35–44.

Harris, K., Aylott, M., Cui, Y., Louttit, J. B., McMahon, N. C., and Sridhar, A. (2013). Comparison of electrophysiological data from human-induced pluripotent stem cell-derived cardiomyocytes to functional preclinical safety assays. *Toxicol. Sci.* **134**, 412–426.

Hirt, M. N., Boeddinghaus, J., Mitchell, A., Schaaf, S., Börnchen, C., Müller, C., Schulz, H., Hubner, N., Stenzig, J., Stoehr, A., *et al.* (2014). Functional improvement and maturation of rat and human engineered heart tissue by chronic electrical stimulation. *J. Mol. Cell. Cardiol.* **74C**, 151–161.

Hoekstra, M., Mummery, C. L., Wilde, A. M., Bezzina, C. R., and Verkerk, A. O. (2012). Induced pluripotent stem cell derived cardiomyocytes as models for cardiac arrhythmias. *Front. Physiol.* **3**, 346.

Huo, J., Kamalakar, A., Yang, X., Word, B., Stockbridge, N., Lyn-Cook, B., and Pang, L. (2016). Evaluation of batch variations in induced pluripotent stem cell-derived human cardiomyocytes from 2 major suppliers. *Toxicol. Sci.* kfw235, 1–14.

Hwang, H. S., Kryshtal, D. O., Feaster, T. K., Sánchez-Freire, V., Zhang, J., Kamp, T. J., Hong, C. C., Wu, J. C., and Knollmann, B. C. (2015). Comparable calcium handling of human iPSC-derived cardiomyocytes generated by multiple laboratories. *J. Mol. Cell. Cardiol.* **85**, 79–88.

Jung, G., Fajardo, G., Ribeiro, A. J. S., Kooiker, K. B., Coronado, M., Zhao, M., Hu, D., Reddy, S., and Kodo, K. (2016). Time-dependent evolution of functional vs. remodeling signaling in induced pluripotent stem cell-derived cardiomyocytes and induced maturation with biomechanical stimulation. *FASEB J.* **30**, 1464–1479.

Kise, H., Nakamura, Y., Hoshiai, M., Sugiyama, H., Sugita, K., and Sugiyama, A. (2009). Cardiac and haemodynamic effects of tacrolimus in the halothane-anaesthetized dog. *Basic Clin. Pharmacol. Toxicol.* **106**, 288–295.

Kuschinsky, K., Lahrtz, H., Lüllmann, H., and van Zwieten, P. A. (1967). Accumulation and release of 3H-digoxin by guinea-pig heart muscle. *Br. J. Pharmacol. Chemother.* **30**, 317–328.

Lee, P., Klos, M., Bollensdorff, C., Hou, L., Ewart, P., Kamp, T. J., Zhang, J., Bizy, A., Guerrero-Serna, G., Kohl, P., *et al.* (2012). Simultaneous voltage and calcium mapping of genetically purified human induced pluripotent stem cell-derived cardiac myocyte monolayers. *Circ. Res.* **110**, 1556–1563.

Lemoine, H., and Overlack, C. (1992). Highly potent beta-2 sympathomimetics convert to less potent partial agonists as relaxants of guinea pig tracheae maximally contracted by carbachol. Comparison of relaxation with receptor binding and adenylate cyclase stimulation. *J. Pharmacol. Exp. Ther.* **261**, 258–270.

Lopez-Izquierdo, A., Warren, M., Riedel, M., Cho, S., Lai, S., Lux, R. L., Spitzer, K. W., Benjamin, I. J., Tristani-Firouzi, M., and Jou, C. J. (2014). A near-infrared fluorescent voltage-sensitive dye allows for moderate-throughput electrophysiological analyses of human induced pluripotent stem cell-derived cardiomyocytes. *AJP Hear. Circ. Physiol.* **307**, H1370–H1377.

Lüllmann, H., and Ravens, U. (1973). The time courses of the changes in contractile force and in transmembfane potentials induced by cardiac glycosides in guinea-pig papillary muscle. *Br. J. Pharmacol.* **49**, 377–390.

MacCoun, R., and Perlmutter, S. (2015). Hide results to seek the truth. *Nature* **526**, 187–189.

Mannhardt, I., Breckwoldt, K., Letuffe-Brenière, D., Schaaf, S., Schulz, H., Neuber, C., Benzin, A., Werner, T., Eder, A., Schulze, T., *et al.* (2016). Human engineered heart tissue: Analysis of contractile force. *Stem Cell Rep.* **7**, 29–42.

McCall, E., Li, L., Satoh, H., Shannon, T. R., Blatter, L. A., and Bers, D. M. (1996). Effects of FK-506 on contraction and Ca2+ transients in rat cardiac myocytes. *Circ. Res.* **79**, 1110–1121.

Milting, H., Janssen, P. M. L., Wangemann, T., Kogler, H., Domeier, E., Seidler, T., Hakim, K., Grapow, M., and Zeitz, O. (2001). FK506 does not affect cardiac contractility and adrenergic response in vitro. *Eur. J. Pharmacol.* **430**, 299–304.

Molenaar, P., Bartel, S., Cochrane, A., Vetter, D., Jalali, H., Pohlner, P., Burrell, K., Karczewski, P., Krause, E. G., and Kaumann, A. (2000). Both beta(2)- and beta(1)-adrenergic receptors mediate hastened relaxation and phosphorylation of phospholamban and troponin I in ventricular myocardium of Fallot infants, consistent with selective coupling of beta(2)-adrenergic receptors to G(s)-protein. *Circulation* **102**, 1814–1821.

Molenaar, P., Christ, T., Hussain, R. I., Engel, A., Berk, E., Gillette, K. T., Chen, L., Galindo-Tovar, A., Krobert, K. A., Ravens, U., *et al.* (2013). PDE3, but not PDE4, reduces ß1- and β2-adrenoceptor-mediated inotropic and lusitropic effects in failing ventricle from metoprolol-treated patients. *Br. J. Pharmacol.* **169**, 528–538.

Mügge, A., Posselt, D., Reimer, U., Schmitz, W., and Scholz, H. (1985). Effects of the beta 2-adrenoceptor agonists fenoterol and salbutamol on force of contraction in isolated human ventricular myocardium. *Klin. Wochenschr.* **63**, 26–31.

Navarrete, E. G., Liang, P., Lan, F., Sanchez-Freire, V., Simmons, C., Gong, T., Sharma, A., Burridge, P. W., Patlolla, B., Lee, A. S., *et al.* (2013). Screening drug-induced arrhythmia events using human induced pluripotent stem cell-derived cardiomyocytes and low-impedance microelectrode arrays. *Circulation* **128**, S3–13.

Pankucsi, C., Varró, A., and Nánási, P. P. (1996). Three distinct components of the negative inotropic action of lidocaine in dog Purkinje fiber. *Gen. Pharmacol.* **27**, 69–71.

Pecha, S., Flenner, F., Söhren, K.-D., Lorenz, K., Eschenhagen, T., and Christ, T. (2015). β1 Adrenoceptor antagonistic effects of the supposedly selective β2 adrenoceptor antagonist ICI 118,551 on the positive inotropic effect of adrenaline in murine hearts. *Pharmacol. Res. Perspect.* **3**, e00168.

Pointon, A., Harmer, A. R., Dale, I. L., Abi-Gerges, N., Bowes, J., Pollard, C., and Garside, H. (2015). Assessment of cardiomyocyte contraction in human-induced pluripotent stem cell-derived cardiomyocytes. *Toxicol. Sci.* **144**, 227–237.

Pousti, A., Deemyad, T., and Malihi, G. (2004). Mechanism of inhibitory effect of citalopram on isolated guinea-pig atria in relation to adenosine receptor. *Hum. Psychopharmacol.* **19**, 347–350.

Qu, Y., and Vargas, H. M. (2015). Proarrhythmia risk assessment in human induced pluripotent stem cell-derived cardiomyocytes using the Maestro MEA platform. *Toxicol. Sci.* **147**, 286–295.

Reiter, M. (1972). Differences in the inotropic cardiac effects of noradrenaline and dihydro-ouabain. *Naunyn. Schmiedebergs. Arch. Pharmacol.* **275**, 243–250.

Schaaf, S., Eder, A., Vollert, I., Stöhr, A., Hansen, A., Eschenhagen, T., Stöhr, A., Hansen, A., and Eschenhagen, T. (2014). Generation of strip-format fibrin-based engineered heart tissue (EHT). *Methods Mol. Biol.* **1181**, 121–129.

Schlepper, M. (1989). Cardiodepressive effects of antiarrhythmic drugs. *Eur. Heart J.* **10(Suppl. E)**, 73–80.

Schotten, U., Ausma, J., Stellbrink, C., Sabatschus, I., Vogel, M., Frechen, D., Schoendube, F., Hanrath, P., and Allessie, M. A. (2001). Cellular mechanisms of depressed atrial contractility in patients with chronic atrial fibrillation. *Circulation* **103**, 691–698.

Scott, C. W., Zhang, X., Abi-Gerges, N., Lamore, S. D., Abassi, Y. A., and Peters, M. F. (2014). An impedance-based cellular assay using human iPSC-derived cardiomyocytes to quantify modulators of cardiac contractility. *Toxicol. Sci.* **142**, 331–338.

Sutko, J. L., and Willerson, J. T. (1980). Ryanodine alteration of the contractile state of rat ventricular myocardium. Comparison with dog, cat, and rabbit ventricular tissues. *Circ. Res.* **46**, 332–343.

Sutko, J. L., Willerson, J. T., Templeton, G. H., Jones, L. R., and Besch, H. R. (1979). Ryanodine: Its alterations of cat papillary muscle contractile state and responsiveness to inotropic interventions and a suggested mechanism of action. *J. Pharmacol. Exp. Ther.* **209**, 37–47.

Tremblay, S., Nigro, V., Weinberg, J., Woodle, E. S., and Alloway, R. R. (2016). A STeady-state head-to-head pharmacokinetic comparison of all FK-506 (Tacrolimus) formulations (ASTCOFF): An open label, prospective, randomized, two arm, three period crossover study. *Am. J. Transplant* **XX**, 1–11.

Tsuboi, M., and Chiba, S. (1999). Effects of lidocaine on isolated, blood-perfused ventricular contractility in the dog. *Heart Vessels* **14**, 289–294.

Uzun, A. U., Mannhardt, I., Breckwoldt, K., Horváth, A., Johannsen, S. S., Hansen, A., Eschenhagen, T., and Christ, T. (2016). Ca(2+)-currents in human induced pluripotent stem cell-derived cardiomyocytes effects of two different culture conditions. *Front. Pharmacol.* **7**, 300.